White Rose Research Online

eprints@whiterose.ac.uk
https://eprints.whiterose.ac.uk
Universities of Leeds, Sheffield and York

Deposited via The University of Leeds.

White Rose Research Online URL for this paper:
https://eprints.whiterose.ac.uk/id/eprint/79994/

Version: Accepted Version

Article:
Lutz, S, Anesio, AM, Jorge Villar, SE et al. (2014) Variations of algal communities cause darkening of a Greenland glacier. FEMS Microbiology Ecology, 89 (2). 402 - 414. ISSN: 0168-6496

https://doi.org/10.1111/1574-6941.12351

Reuse
Items deposited in White Rose Research Online are protected by copyright, with all rights reserved unless indicated otherwise. They may be downloaded and/or printed for private study, or other acts as permitted by national copyright laws. The publisher or other rights holders may allow further reproduction and re-use of the full text version. This is indicated by the licence information on the White Rose Research Online record for the item.

Takedown
If you consider content in White Rose Research Online to be in breach of UK law, please notify us by emailing eprints@whiterose.ac.uk including the URL of the record and the reason for the withdrawal request.

UNIVERSITY OF LEEDS
University of Sheffield
UNIVERSITY of York

RESEARCH ARTICLE

Variations of algal communities cause darkening of a Greenland glacier

Stefanie Lutz[1], Alexandre M. Anesio[2], Susana E. Jorge Villar[3] & Liane G. Benning[1]

[1]School of Earth & Environment, University of Leeds, Leeds, UK; [2]Bristol Glaciology Centre, School of Geographical Sciences, University of Bristol, Bristol, UK; and [3]Area de Geodinamica Interna, Facultad de Humanidades y Educacion, Universidad de Burgos, Burgos, Spain

Correspondence: Stefanie Lutz, School of Earth & Environment, University of Leeds, Leeds LS2 9JT, UK.
Tel.: +44 (0)113 34 33647;
fax: +44 (0)113 34 35259;
e-mail: s.lutz@leeds.ac.uk

Received 11 December 2013; revised 11 April 2014; accepted 24 April 2014.

DOI: 10.1111/1574-6941.12351

Editor: John Priscu

Keywords
snow and ice algae; albedo; pigments; melting; Greenland; microbial habitats.

Abstract

We have assessed the microbial ecology on the surface of Mittivakkat glacier in SE-Greenland during the exceptional high melting season in July 2012 when the so far most extreme melting rate for the Greenland Ice Sheet has been recorded. By employing a complementary and multi-disciplinary field sampling and analytical approach, we quantified the dramatic changes in the different microbial surface habitats (green snow, red snow, biofilms, grey ice, cryoconite holes). The observed clear change in dominant algal community and their rapidly changing cryo-organic adaptation inventory was linked to the high melting rate. The changes in carbon and nutrient fluxes between different microbial pools (from snow to ice, cryoconite holes and glacial forefronts) revealed that snow and ice algae dominate the net primary production at the onset of melting, and that they have the potential to support the cryoconite hole communities as carbon and nutrient sources. A large proportion of algal cells is retained on the glacial surface and temporal and spatial changes in pigmentation contribute to the darkening of the snow and ice surfaces. This implies that the fast, melt-induced algal growth has a high albedo reduction potential, and this may lead to a positive feedback speeding up melting processes.

Introduction

The cryosphere covers about 10% of Earth's surface and has only recently been recognized as a biome (Anesio & Laybourn-Parry, 2012). Although lower in cell numbers than more temperate environments, many microorganisms (both autotrophs and heterotrophs) survive and even thrive in/on snow and ice. Glacial surfaces are usually assumed to be rather homogenous in terms of their microbiology, but they are composed of a range of distinct microbial habitats that include snow, bare ice and cryoconites (Anesio & Laybourn-Parry, 2012). Importantly, on snow and ice surfaces, various studies have shown that primary productivity is limited usually by light and nutrient availability (Remias *et al.*, 2005; Stibal *et al.*, 2007; Leya *et al.*, 2009; Yallop *et al.*, 2012; Takeuchi, 2013).

Algal blooms colouring snow and ice surfaces are abundant on glacial surfaces and have been known for a long time (first reported by the ancient Greek Aristotle; Gentz-Werner, 2007), and they have been described from many cryospheric settings (Thomas & Duval, 1995; Leya *et al.*, 2000, 2004; Müller *et al.*, 2001; Williams *et al.*, 2003; Takeuchi *et al.*, 2006; Lütz *et al.*, 2009; Duval *et al.*, 2010; Fujii *et al.*, 2010). In order to adapt to the harsh conditions on snow and ice surfaces (e.g. high irradiation, low nutrient concentrations), algae are equipped with a suite of protective biomolecules, for instance pigments (Müller *et al.*, 1998; Remias *et al.*, 2005). Dominant species on snow fields belong to the unicellular *Chlamydomonaceae*, with the most prominent representative being *Chlamydomonas nivalis*, a species that needs to be treated as a collective taxon (Leya 2004). Green snow is assumed to be caused by young, trophic stages of snow algae, whereby more mature and carotenoid-rich resting stages result in all shades of red snow. The physiology, morphologies and ecological traits of snow algal communities have been described in various studies (Hoham & Duval, 2001; Leya *et al.*, 2004; Remias *et al.*, 2005, 2013).

Ice algae on the other hand have only recently been described and, so far, seem to have a less complex life cycle, where they thrive on bare glacial ice as immotile

© 2014 Federation of European Microbiological Societies.
Published by John Wiley & Sons Ltd. All rights reserved

FEMS MICROBIOLOGY ECOLOGY

(often chained up) cells and only rarely form spores (Remias *et al.*, 2012a; Yallop *et al.*, 2012). Their pigmentation has recently been identified as the brownish pigment purpurogallin carboxylic acid-6-O-b-D-glucopyranoside (Remias *et al.*, 2012b), which causes a less distinct grey coloration of the ice surface. Ice algae belong to the *Zygnematophyceae* and the most described species are *Ancylonema nordenskiöldii* and *Mesotaenium bergrenii*.

In addition to snow and ice, cryoconite holes – cyanobacteria dominated water-filled holes – covering about 1–10% of glacial surfaces are also known as hotspots for nutrient cycling. Compared with snow and ice, cryoconite holes have been by far the more extensively studied ice surface habitats (e.g. Stibal *et al.*, 2008; Hodson *et al.*, 2010; Telling *et al.*, 2011; Anesio & Laybourn-Parry, 2012).

In most of the studies discussed above, single surface glacial habitats (e.g. either snow, or ice or cryoconite holes) and in most cases only individual species or adaptation strategies have been addressed. However, integrating microbial ecological traits of all habitats and adaptations on a full glacial scale is lacking. Here, we present results from a comprehensive and complementary study of the microbial ecology of Mittivakkat glacier in south-east Greenland, a glacier whose biology has not been investigated yet. Our field work period (July 2012) was characterized by extremely high temperatures and an anomalous, stagnant ridge of warm air over Greenland, which caused the most extreme melting event of the Greenland Ice Sheet (GrIS) in the last 150 years (Nghiem *et al.*, 2012). During the summer of 2012, Mittivakkat glacier experienced its fourth largest mass loss year since 1995 (Hanna *et al.*, 2012; Mernild *et al.*, 2012; Tedesco *et al.*, 2013), most probably speeding up physical and microbial processes. To our knowledge, this is the first report detailing the entire microbial ecology of a glacial surface ecosystem and also addressing the fast temporal and spatial changes in algal communities and the adaptive inventories of the various algal species and linking these to the resulting effects on the changes in physical properties of the glacier.

Materials and methods

Field site

Mittivakkat glacier (MIT), located in south-east Greenland just below the Arctic Circle (65.6°N; 37.8°W), is a polythermal glacier with low mean annual temperatures of −1.7 °C (Cappelen *et al.*, 2011). MIT is located on Ammassalik Island and is an independent glacier separated from the Greenland Ice Sheet. The bottom of the glacier is located at 128 m a.s.l, the terminus at 180 m a.s.l. and its summit at 880 m a.s.l. The surrounding bedrock consists mainly of gneisses and gabbro-anorthosite intrusions (Escher & Watt, 1976). Between the 6th and 23rd of July 2012, we carried out an in-depth snow, ice and melt water sampling campaign that was complemented by a series of *in situ* metabolic and irradiation measurements over an area of *c.* 1 km^2 (Fig. 1) of MIT. We aimed at characterizing the changes in the glacial ecology during a single melting season. This was particularly pertinent due to the extremely high melting rates in the summer of 2012 (Mernild *et al.*, 2012; Hanna *et al.*, 2013). Hanna *et al.* (2013) carried out a detailed mass balance study in the 2 weeks following our field campaign on Mittivakkat glacier. They have shown that the glacier experienced its fourth largest mass loss since 1995 during summer of 2012. In the 3 weeks prior to their detailed measurements, our monitoring of the surface changes of MIT showed a move of the snow line up from *c.* 128 to 250 m a.s.l. During our campaign and based on visual observations, we surveyed and defined several distinct microbial glacial surface habitats that are considered to be highly representative of the whole glacial surface: clean snow (white snow with no visual presence of particles), green snow (light to dark green and depth pervasive distribution of colour), red snow (variably dense light pink to dark red pigmentation that was usually only forming a thin covering on white snow), biofilms (wet snow at snow-ice melting interfaces), clean ice (white ice with no visual presence of particles), grey ice (light grey to dark grey ice covered with dark particles), cryoconite holes (1–50 cm large usually rounded or elongated and variably deep holes filled with sediment) and glacial run-off (melt rivers and channels). In each of these habitats (except for glacial run-off where only one sample was collected), we collected various samples for microbial, mineralogical and geochemical analyses. Throughout the field campaign, we collected a total of 24 samples which represented different habitats that developed with time at various sites (Fig. 1 and Table 1). A true time resolved sampling could not be carried out as the snow-melt was fast and the aspect of sampling spots varied substantially even within 24 h. Below, we only briefly describe the main field and laboratory approaches, and the full details are given in the Supporting Information.

Field measurements

A total of 24 samples – labelled MIT-2 to MIT-25 – was collected (MIT-1 represents a blank sample that we processed in the same way like all other samples). To obtain a good spatial and temporal representation of the glacial surface habitats, two clean snow, two green snow, nine red snow, three biofilm, one clean ice, three grey ice,

© 2014 Federation of European Microbiological Societies.
Published by John Wiley & Sons Ltd. All rights reserved

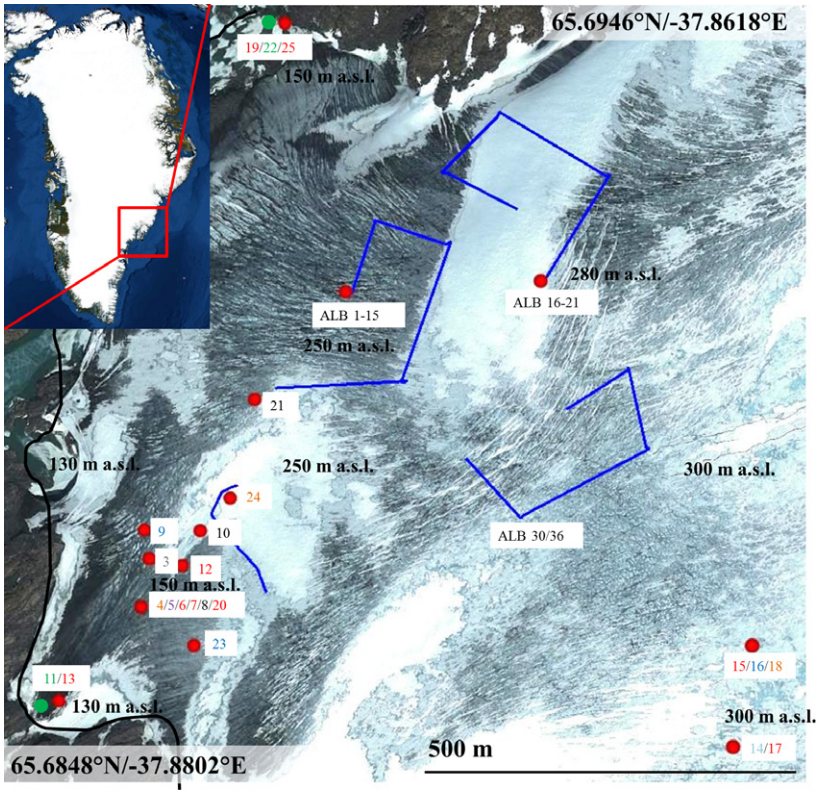

Fig. 1. Mittivakkat Glacier in SE-Greenland showing the distribution of our sampling and measurement sites; blue lines represent albedo survey traverses (ALB). Black line delineates the bottom of the glacier. Numbers and colours correspond to the sample numbers MIT-2 to MIT-25 (grey = white snow, green = green snow, red = red snow, light blue = clean ice, dark blue = grey ice, brown = biofilms, black = cryoconite holes, purple = run-off. Image source: Google Earth (August 2012).

Table 1. Coordinates, sample habitat categorization and field measurements for each sampling site on Mittivakkat glacier (MIT-2 to MIT-25)

Sample no.	Sample description	Collection date July 2012	GPS location (24 H, UTM)	Elevation (m a.s.l.)	pH	Temp. (°C)	Cond. (μM)	PAR (W m^{-2})	UV-A (W m^{-2})	UV-B (W m^{-2})	Albedo (%)
MIT-2	Clean snow #1	9th									
MIT-3	Clean snow #2	9th	0551579E, 7285535N	190	7.05	1.7	0	346	40.2	1.14	83
MIT-4	Biofilm #1	10th	0551567E, 7285460N	155	6.39	0	0	131	17.8	0.72	
MIT-5	Surface run-off	10th	0551567E, 7285460N	155	5.59	0	0	195	27.0	1.01	
MIT-6	Red snow #1	10th	0551567E, 7285460N	155	5.31	0	0	191	24.4	1.02	
MIT-7	Red snow #2	10th	0551567E, 7285460N	155	5.67	0	2	204	28.1	1.13	
MIT-8	Cryoconite hole #1	10th	0551567E, 7285460N	155							
MIT-9	Grey ice #1	12th	0551571E, 7285579N	196				276	35.3	1.39	
MIT-10	Cryconite hole #2	12th	0551659E, 7285580N	196	5.84	0	0	275	34.4	1.34	
MIT-11	Green snow #1	12th	0551435E, 7285308N	128	5.49	0	0	182	20.3	0.61	39
MIT-12	Red snow #3	12th	0551631E, 7285526N	204	5.73	0	0	318	38.1	1.37	
MIT-13	Red snow #4	12th	0551435E, 7285308N	128	5.83	0.2	0	182	20.3	0.61	
MIT-14	Clean ice #1	14th	0552441E, 7285291N	294				356	41.0	2.13	63
MIT-15	Red snow #5	14th	0552463E, 7285438N	299	5.73	0	0				
MIT-16	Grey ice #2	14th	0552463E, 7285438N	299	5.46	0	0				39
MIT-17	Red snow #6	14th	0552441E, 7285291N	294	5.48	0	0	356	41.0	2.13	57
MIT-18	Biofilm #2	14th	0552463E, 7285438N	299	5.62	0	0				23
MIT-19	Red snow #7	17th	0551778E, 7286368N	150	4.68	0.7	0	345	46.2	1.54	39
MIT-20	Red snow #8	10th	0551567E, 7285460N	155	5.31	0	0	191	24.4	1.02	
MIT-21	Cryoconite hole #3	17th	0551741E, 7285782N	233	6.35	0.1	0				27
MIT-22	Green snow #2	17th	0551778E, 7286368N	150	5.02	0	0	345	46.2	1.54	48
MIT-23	Grey ice #3	19th	0551651E, 7285404N	195							38
MIT-24	Biofilm #3	19th	0551705E, 7285631N	204	5.75	0	0				20
MIT-25	Red snow #9	17th	0551778E, 7286368N	150							

PAR, photosynthetic active radiation.

© 2014 Federation of European Microbiological Societies.
Published by John Wiley & Sons Ltd. All rights reserved

three cryoconite holes and one run-off sample were randomly collected over the full monitoring area of 1 km^2. Due to the extremely fast snow-melting rates (Hanna *et al.*, 2013), re-sampling of the same habitat at the exact same site was not feasible for the snow or ice habitats. Even from 1 day to another melting changed most habitats dramatically and often led to the transformation of one habitat into another (e.g. clean snow→red snow or red snow/biofilm→grey ice). Thus, a time resolved sampling of the same habitat on the same site was not possible, and samples were collected at different sites taking into account the habitat definitions described above.

At each sampling point prior to sampling, the snow temperature (upper few cm), pH and conductivity were measured *in situ* using a multi-meter (HI 98129; Hanna instruments). In all snow habitats and the run-off, pH and conductivity measurements were taken after allowing the multi-metre to equilibrate in the upper 2–3 cm of the respective habitat. For the clean and grey ice habitats, this was achieved by melting a few ice chips on site and measuring the values with the multi-metre. Furthermore, at each site (as well as during a large survey, Table S1), irradiation was measured with a radiometer with specific Photosynthetic active radiation (PAR), UVA and UVB sensors (SolarLight PMA2100). Albedo was calculated by taking the ratio of reflected to incident radiation (400–700 nm range) and measuring the values always in the same position to the sun. There was no cloud cover during the whole field campaign. Measurements were taken with the sensors held at 30 cm above the snow surface (field of view 160°, effective measurement area 0.5 m^2) and by first pointing the sensor upwards (incident radiation) and then towards the snow/ice surface (reflected radiation). Five measurements for incident and reflected radiation were taken each. The error of the measurement (standard deviation) was below 10%. The rate of snowmelt was monitored over an area of 80 m^2 with tagged poles inserted into the snow and down to the ice layer, with measurements taken every 1–2 days (at site MIT-3). Snow, ice and water samples were collected either in sterile 50 mL centrifuge tubes (for all inorganic analyses) or in 250 mL ashed glass jars (for organic analyses). All samples were kept cold (in packed snow) and processed within 24 h (see below). To evaluate the bulk community activity and the proportion of autochthonous carbon production and consumption, measurements of changes in O_2 concentrations over 24–48 h in light and dark bottles were taken at three sites (MIT 3/11/13). At the end of each field day, 1 mL of untreated snow, ice, biofilm and cryoconite samples was imaged using a portable light microscope (100 and 400× magnification) and snow (spherical cells) and ice algal (desmids) cells were counted on a hemocytometer. A minimum of 150 cells or 300 μL of sample was counted. All samples were counted in duplicates.

Aqueous and solid phase analyses

All samples were processed within 24 h of sampling to preserve solutions and solids for various analyses. Full details of the various sample handling stages are given in the Supporting Information. Processed and preserved samples were returned to the UK either cold or frozen. Aqueous samples were analysed for anion and cation compositions using ion chromatography (IC) and for trace metals using inductive coupled plasma mass spectrometry (ICP-MS). Microbial and inorganic debris were imaged using light, scanning electron and transmission electron microscopy (LM, SEM and TEM, respectively). Functional group distribution and mineralogy were characterized using vibrational spectroscopy (Fourier transform infrared, FTIR, and Raman) and X-ray diffraction (XRD) methods with the FTIR focussing on the ratios of lipids and proteins to carbohydrates, the XRD on the mineral characterization and the Raman on the major differences in organic compounds and the cross-confirmation of mineralogical characteristics. For the characterization of the chlorophyll to carotenoid ratios in the snow algae samples, high pressure liquid chromatography (HPLC) was used on extracted snow algal pigments and data are presented as ratios of carotenoids to chlorophyll *a* (Chl *a*). Full details for all methods are provided in the Supporting Information.

Results

Physical change of the glacial surface and change in algal communities

At the beginning of the field season (6th of July), the glacier was fully snow-covered and no particles were macroscopically visible on the snow. After a couple of days (8th of July), concomitant with a dramatic ambient air temperature increase (*c.* 5 °C over a few days, based on temperature loggers of the Department of Geosciences and Natural Resource Management, University of Copenhagen), which induced the onset of intense melting, two green snow patches (covering each *c.* 20 m^2 and reaching down to almost the bare ice layer, i.e. 20–40 cm) formed at the bottom of the glacier (*c.* 130 m a.s.l., Figs 1 and 2a). Within the following 2 days (10th of July), thin layers of red snow (Figs 1 and 2a and b top right) developed in patches initially close to the green snow. Gradually within the next 2 weeks of observation (10th to 23rd of July), numerous and fast changing light to dark red snow patches formed

© 2014 Federation of European Microbiological Societies.
Published by John Wiley & Sons Ltd. All rights reserved

on the snow-covered glacier. The distribution of these red snow patches progressed upwards with the snow line from the bottom of the glacier to increasingly higher levels (from 128 to *c.* 350 m a.s.l.; Figs 1 and 2a). Following the onset of melting, we estimated that, at various times during our sampling season, between 5% and 50% of the 1-km^2 surveyed area was covered by a thin layer (often < 1–2 mm thick) of red snow. This estimate was based on our observations during the albedo surveys (totalling 700 measurements of albedo) as well as visual estimates during the initial and end field site surveys. It is worth mentioning that the distribution of these red snow patches (and indeed of most snow or ice habitats) was highly patchy and both temporally and spatially heterogeneous not just in distribution but also in terms of patch size, with patches as small as 0.5 m^2 or as large as 30 m^2. Once melting of the snow occured, small water pools formed at the interface between snow and ice habitats (Fig. 2b bottom left and c). These were dominated by brownish-blackish biofilms and were characterized by extremely high microbial contents and photosynthetic activity (Figs 2b bottom left and 3) but also likely by the presence of high concentrations of inorganic impurities (dust, black carbon, etc.) that accumulated due to the melting snow. On areas where all snow had melted, the bare ice surface was either extremely clean (clean ice habitat, mostly in areas of slightly higher topography) or it became covered with greyish mottled particles (grey ice habitat) and variably sized cryoconite holes. At the end of the field season (25th of July), we estimate (based on the 1 km^2 survey area) that *c.* 70–90% of the glacier < 350 m a.s.l. was snow free and dominated by grey ice interspersed with cryoconite holes. At the end of our field observations on Mittivakkat glacier, clean snow without any visually distinctive microbial presence could only be found above 350 m a.s.l.

These melt-driven spatial and temporal changes in the macroscopic aspect of the glacier surfaces were accompanied by a clear change in the algal community, distribution and abundance (Fig. 2; Table 2). The algal species that dominated each observed habitat differed in shape, colouring and density, and each habitat dramatically changed in occurrence and spatial distribution of microorganisms as the melt season progressed. Species identification by light microscopy showed that spherical,

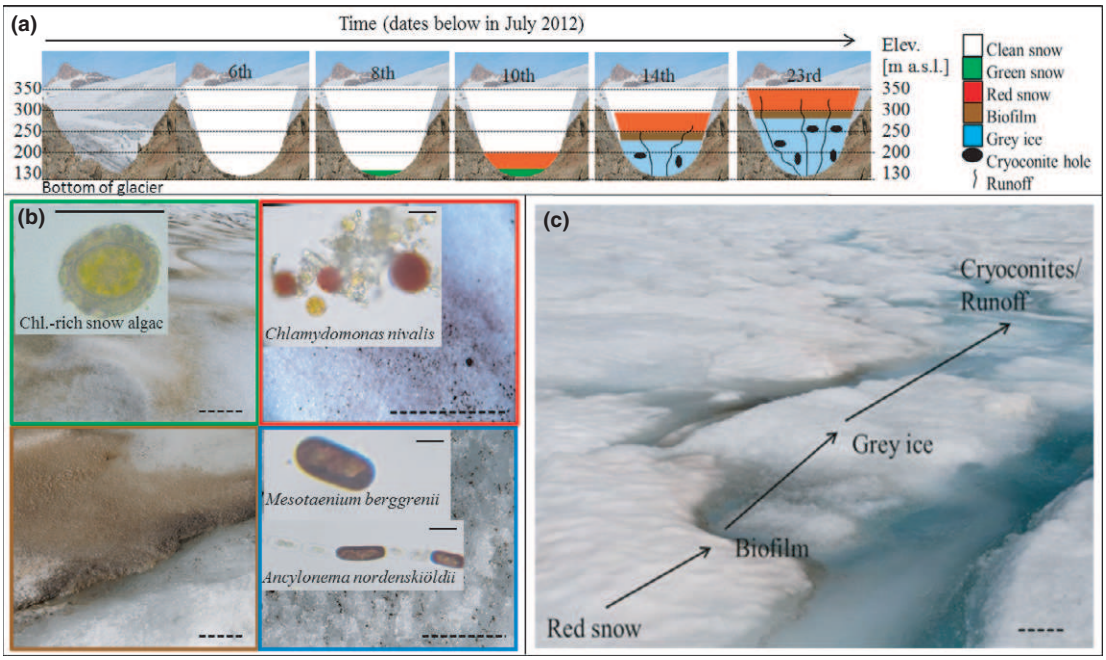

Fig. 2. Schematic representation of the changes in the spatial (elevation) and temporal (time from left to right) distribution in microbial habitats during the field season. (a) and (c) show the microbial habitats and (b) showing various algal communities observed on glacier; (b top left image) shows the green snow sample MIT-22 with the corresponding chlorophyll-rich green algae; (b top right image) shows sample MIT-19 and the spherical yellow and red snow algae *Chlamydomonas nivalis*; (b bottom left image) shows a biofilm (sample MIT-4) likely producing O_2 bubbles and its corresponding mixed community of spherical snow algae and filamentous ice algae and (b bottom right image) shows a grey ice sample (MIT-9) with the corresponding ice algal strains. (c) shows the transition between habitats in a relatively small area. Solid scale bar: 10 μm, dotted scale bar: 10 cm. Approximate elevation lines were added in (a) as a guide to the eye only; in (a) snow and ice habitats are represented by the different colours, while cryoconite holes and the run-off are represented by the graphical symbols in the legend at right.

© 2014 Federation of European Microbiological Societies.
Published by John Wiley & Sons Ltd. All rights reserved

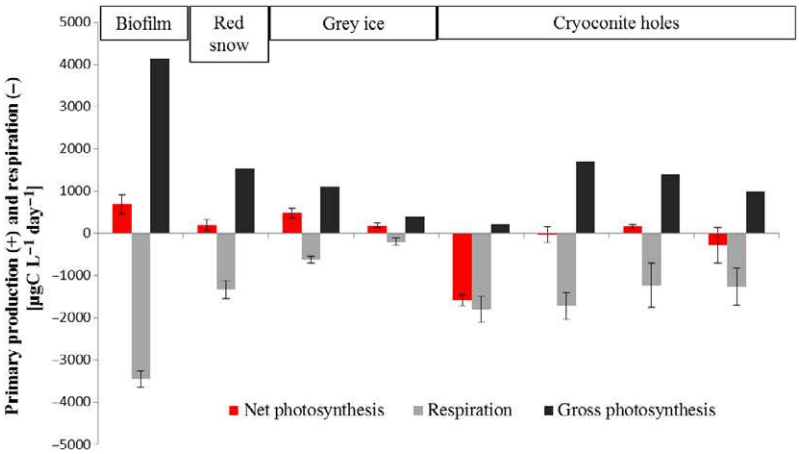

Fig. 3. Microbial activity determined as net photosynthesis rates for all measured sample types: biofilm, cryoconites (four sample sets), ice algae from the grey ice (two sample sets) and red snow algae; each bar represents the average of three individual measurements with the error bars shown.

Table 2. Cell counts from the on-site light microscopic measurements showing the ranges that characterized the snow (spherical cells) and ice algae (filamentous cells) in each habitat (see also Fig. 2)

Category	Sample no.	Snow algae (cells mL^{-1})	Ice algae (cells mL^{-1})	Ratio snow/ ice algae
Green snow (n = 1)	MIT-22	4245	ND	ND
Red snow n = 8)	MIT-6	8580	ND	ND
	MIT-7	25 800	26 210	1 : 1
	MIT-12	12 900	232	56 : 1
	MIT-13	11 900	190	63 : 1
	MIT-15	27 000	13 886	2 : 1
	MIT-17	1770	6076	1 : 3
	MIT-19	5900	ND	ND
	MIT-20	52 000	8664	6 : 1
Average		18 231	9210	2 : 1
Grey ice (n = 3)	MIT-9	409	5306	1 : 13
	MIT-16	6920	19 991	1 : 3
	MIT-23	1843	7057	1 : 4
Average		3057	10 785	1 : 4
Biofilm (n = 3)	MIT.4	1860	60	31 : 1
	MIT-18	12 400	52 600	1 : 4
	MIT-24	48 000	368 000	1 : 8
Average		20 753	140 220	1 : 7
Cryoconite holes (n = 3)	MIT-8	9150	16 950	1 : 2
	MIT-10	480	20	24 : 1
	MIT-21	270	ND	ND
		3300	8485	1 : 3
Run-off (n = 1)	MIT-5	1.43	0.28	5 : 1

ND, not detected.

chlorophyll-rich green and carotenoid-rich red snow algae cells were predominantly represented by resting cysts of the unicellular snow algae *C. nivalis*, while ice algae were represented either by the filamentous *A. nordenskiöldii* (predominantly chains) or by the unicellular *Mesotaenium berggrenii* (Fig. 2b). Both algal types (snow and ice algae) were found in snow and ice samples, but were dominant in their respective habitats. The biofilms, which formed at the snow–ice interface, were characterized by a broad range of snow to ice algae ratios (Table 2) and showed the highest concentrations of mineral/organic debris (algae and bacteria), and the overall density of snow and ice algal cells in these samples was far higher compared with other algal samples.

Field measurements

The snow-melting progressed fast during our field season. We measured surface melting rates of 5 cm of snow per day, which over the monitored 1-km^2 area equates to 0.05 km^3 of snow loss per day. Despite this, the snow and ice temperature at each collection site varied only over a narrow range from 0 to 1.7 °C. The pH varied from slightly acid (4.7–5.8) for algal sites to near neutral (5.8–6.4) for biofilms and cryoconite holes to neutral (7.05) for clean snow. The pH of the run-off fell within the slightly acidic pH range (5.6). PAR measurements at the sampling sites ranged from 131 to 356 W m^{-2}, UV-A from 17.8 to 46.2 W m^{-2} and UV-B from 0.61 to 2.13 W m^{-2}, while albedo at the sampling sites and during the albedo survey (averages in Table 3 and all measurements in Supporting Information, Table S1) clearly changed from habitat to habitat. The difference in albedo from the clean (75%) to red snow (*c.* 49%) and to biofilms (20%) is attributed here to a clear link to increased pigmentation and mineral contents (see below). However, a quantitative evaluation of the relative contribution of other impurities such as inorganic dust, other organic matter, black carbon and other changes in physical parameters of snow and ice (i.e. grain size, water contents) were not specifically quantified in this study and still require further investigations.

© 2014 Federation of European Microbiological Societies.
Published by John Wiley & Sons Ltd. All rights reserved

Table 3. Average albedo values (in %), based on > 700 measurements, see Table S1) for habitats identified on Mittivakkat and comparisons with literature data from the few other glacial settings where similar habitats were evaluated

Category	This study	Other studies
Clean snow	75 ± 5	89.3 ± 1.8 (fresh)* 58.0 ± 5.5 (older)*
Clean ice	58 ± 8	59 ± 1†
Red snow	49 ± 8	45.5 ± 1.7–51.0 ± 6.6%*
Green snow	44 ± 4	
Grey ice	35 ± 10	35 ± 1†
Run-off	30 ± 4	
Cryoconite holes	23 ± 15	
Biofilm	20 ± 4	

*Thomas & Duval (1995).
†Yallop *et al.* (2012).

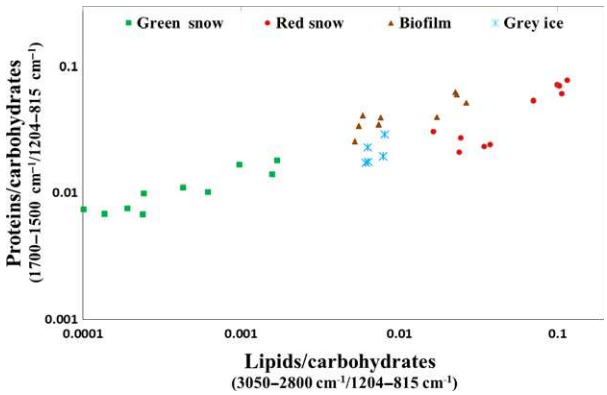

Fig. 4. Ratios of functional groups of protein, lipids and carbohydrates of the different habitats.

The measured net photosynthesis rates (i.e. the difference between gross photosynthesis and community respiration) of the red snow, biofilm and grey ice samples all showed positive trends with the highest values measured for the biofilm sample (Fig. 3). Cryoconite holes were the only habitat with negative values. These results suggest an accumulation of organic matter in all glacial habitats, except for the cryoconite holes, which at this time in the melting season seem to be primarily a location for net consumption of organic matter. Part of this net consumption is also likely derived from organic matter produced in the red and green snow or the grey ice habitats.

Inorganic aqueous and solid analysis

Aqueous analysis (Table S2) revealed at all sites and for all cations and anions concentration values that were mostly low (< μg mL^{-1}) No major differences between sites regardless of microbial presence or absence were observed. Samples contained not just biological components, but also dust debris and the prevailing minerals in each sample, determined by XRD, were quartz, plagioclase, smectite, mica, amphibole and chlorite. These are all minerals that are low in nutrients (e.g. low in P, K, Mg) and are extremely slowly weathered, thus representing poor sources of nutrients for the prevailing microbial communities. Most of these minerals were confirmed through Raman analyses which also identified the presence of black carbon, as well as traces of haematite, limonite and microcline in some samples (Table S3a).

Electron microscopy

Within each algal type, electron imaging revealed large variations in morphological characteristics (Figs S2 and S3). For snow algae, we found a range of morphologies including fairly smooth cells with no or few nipples, cells with uniformly distributed nipples, cells with wave-like surface patterns, shrivelled cells (likely due to sample drying and instrument vacuum) and cells with mucilage sheets.

Organic inventory and functional group distributions

Unfortunately, due to a sample processing error, the DOC/DIC values could not be used and thus the dissolved carbon fluxes between different communities and off the glacier are not available. However, from the vibrational spectroscopic data, we can gain an insight into the changes in prevailing organic compounds in the different algal habitats. The peak area ratios derived from the bulk FTIR data revealed an increasing trend of higher protein/carbohydrate and lipid/carbohydrate ratios from green snow over grey ice and biofilms to red snow (Fig. 4). A series of organic compounds representing among others specific carotenoid C-C bands and chlorophyll bands were clearly identified at the single-cell level by Raman spectroscopy. However, an unambiguous assignment to specific carotenoids could not be carried out, as peak positions even for the same carotenoid band varied from cell to cell even within the same class of cell (see Supporting Information and Table S3b). In addition, it has been recently shown that even small variation in conformation in the carotenoids can affect band positions dramatically (de Oliveira *et al.*, 2010).

Pigment composition

Chlorophyll and carotenoid contents were analysed for all collected samples but only quantified for snow samples as the used method is optimized for these samples. In all snow algae samples, chlorophyll *a* and *b* and the primary

© 2014 Federation of European Microbiological Societies.
Published by John Wiley & Sons Ltd. All rights reserved

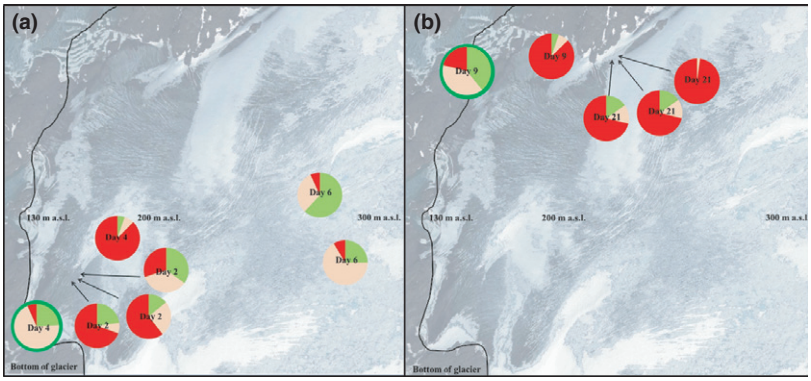

Fig. 5. Overview of pigment ratios in snow algae on Mittivakkat glaciers and spatial (a) and temporal (b) differences. Green portions of each pie chart represents chlorophyll *a* and *b* contents (Chl's), light red primary (pri. Car) and dark red secondary (sec. Car) carotenoids; the two pie charts with dark green rings represent the two green snow samples, all others are red snow samples. Days represent sampling days after the start of the field campaign.

carotenoids neoxanthin, lutein, β-carotene, violaxanthin, zeaxanthin and antheraxanthin were identified in the HPLC traces. The only secondary carotenoid identified was astaxanthin and its fatty acid ester derivatives (Bidigare *et al.*, 1993). The ratios of chlorophyll *a* to primary and secondary carotenoids and their spatial and temporal variations on Mittivakkat glacier are shown in Table 4 and Fig. 5. It is worth noting that samples collected at the onset of melting and snow colonization (MIT-6/7/11/19/20/22), as well as samples collected higher up the glacier (latest melting onset, MIT-15/17) are characterized by higher chlorophyll and primary carotenoid contents, whereas samples collected about a week later (MIT-25, ALB-22/23/24) contained a much large proportion of secondary carotenoids (Fig. 5a and b). Among these, specifically astaxanthin, as well as an increasing esterification resulting in astaxanthin mono- and di-esters, was evident. Furthermore, in these later collected samples, the trans-configuration of astaxanthin was prevalent over the cis-configuration (Table 4). However, interestingly in the green snow sample MIT-11, collected at the beginning of the melting, only traces of astaxanthin were present, whereas the second green snow sample MIT-22, collected a few days later at a different location (Fig. 1), already contained higher amounts of astaxanthin. Despite the large variance in contents and nature of carotenoids among the different red snow samples, no trend could be established for the xantophyll cycle pigments. Pigment analysis of the clean snow samples resulted in only small peaks for chlorophyll and none for carotenoids (not quantified).

Discussion

During the extremely fast 2012 melting season on Mittivakkat glacier (Hanna *et al.*, 2013), our data revealed that snow and ice algae covered a substantial area of the glacial surface and that they had a potential strong influence on both local and downstream physical and biological glacial surface processes. Snow and ice algae are important primary colonisers and carbon producers in the low nutrient snow and ice fields and due to their coloration they have a major impact on snow and ice albedo with reductions down to 20% compared with albedo of fresh snow of 75%. Albedo values often also contain contributions from other non-algal impurities (mineral dust, black carbon, etc.), and these contributions need to be further investigated. However, this was beyond the scope of this paper.

With respect to cell transfer between habitats and although the microbial biomass in cryoconite holes is dominated by heterotrophic bacteria and cyanobacteria (Säwström *et al.*, 2002; Christner *et al.*, 2003; Edwards *et al.*, 2010), our cell counts show that algal cells are washed into cryoconite holes, becoming an important organic matter source for the prevalent community. Cryoconite holes, in turn, are a dominant habitat after the snow-melt in the ablation zone of glaciers and can be self-sustainable and regarded as hot spots for nutrient cycling. However, we hypothesize that both snow and ice algal communities have an important role in supporting cryoconite communities.

Change in life signals

We have shown that snow and ice algae exhibit very different life cycles and cytostructural adaptation strategies (Fig. 4). Green snow, which is dominated by chlorophyll-rich snow algae cells, showed lowest protein and lipid content in relation to carbohydrates. On the other hand, the more mature red algal stage is characterized by incorporation of large amount of storage compounds such as lipid bodies in which pigments are stored (Remias *et al.*, 2005). Late stage spore formation is also accompanied by thickening of the cell walls, mainly composed of glycoproteins, which are also the main compound of mucilage sheets in the spores (Siddiqui & Cavicchioli, 2006). In contrast, ice algae species have thin cell walls and seem

© 2014 Federation of European Microbiological Societies.
Published by John Wiley & Sons Ltd. All rights reserved

Table 4. Chlorophyll and carotenoid analyses for green and red snow samples shown as area ratios normalized to chlorophyll *a*. Note that the red sample set also includes samples that were collected during the albedo survey (ALB samples); for these samples only coordinates, albedo and pigment data is available; shown in grey are total chlorophylls and total primary and secondary carotenoids

Chl *a* = 1	Neo	Vio	trans-Ast	cis-Ast	Ant	Lut	Zea	Chl *b*	trans-Ast mono-esters	cis-Ast mono-esters	trans-Ast di-esters	cis-Ast di-esters	All Ast	Chlorophylls	Primary carotenoids	Secondary carotenoids
Green snow																
MIT-11	0.00	0.00	0.00	0.00	0.00	3.56	0.00	0.24	0.34	0.00	0.00	0.00	0.34	1.24	3.56	0.34
MIT-22	0.48	0.00	0.00	0.00	0.00	1.11	0.00	1.37	1.09	0.19	0.00	0.00	1.28	2.37	2.41	1.28
Red snow																
MIT-6	0.09	0.05	1.05	0.11	0.03	0.86	0.31	0.19	1.83	0.64			3.63	1.19	0.39	3.63
MIT-7	0.05	0.11	3.99	0.67	0.05	1.43	0.57	0.26	0.55	0.21			5.42	1.26	2.26	5.42
MIT-12	0.14	0.16	2.37	0.41	0.28	0.71	0.22	0.15	6.30	3.52	4.60	1.68	18.88	1.15	1.51	18.88
MIT-15	0.01	0.05	0.08	0.00	0.03	0.40	0.05	0.17	0.03	0.02			0.13	1.17	0.59	0.13
MIT-17	0.04	0.43	0.37	0.00	0.45	1.70	0.69	0.30	0.08	0.00			0.45	1.30	3.44	0.45
MIT-19	0.04	0.04	0.20	0.04	0.00	0.60	0.06	0.21	0.27	0.17			0.68	1.21	0.76	0.68
MIT-20	0.10	0.09	0.75	0.12	0.04	0.98	0.17	0.39	0.23	0.09			1.19	1.39	1.39	1.19
MIT-25	0.04	0.02	0.84	0.13	0.00	0.66	0.28	0.15	9.26	5.11	2.55	1.55	19.44	1.15	1.66	19.44
ALB-22	0.05	0.08	0.18	0.03	0.01	0.69	0.09	0.22	1.89	0.64	2.95		5.69	1.22	1.07	5.69
ALB-23	0.07	0.13	0.34	0.00	0.00	1.16	0.35	0.19	5.39	3.79	17.26	16.24	43.02	1.19	2.01	43.02
ALB-24	0.40	0.23	2.57	0.21	0.00	5.66	0.00	0.24	45.62	41.74	131.63	224.65	446.42	1.24	8.60	446.42

not to require equivalent biomolecular protection, which would explain the lower relative lipid and protein content found in the ice habitats by our study. This could also be due to a shorter and less complex life cycle of ice algae, which still remains unknown. As biofilms are a mixture of snow and ice algae, they showed intermediate levels of lipid and proteins. Whether the intermediate ratios also indicate better protection from harsh conditions (e.g. high irradiation) due to the protective water layer and a better nutrient supply due to the adhering matrix still needs to be further investigated.

Although snow algae pigmentation has been extensively studied (Müller *et al.*, 1998; Remias *et al.*, 2005, 2010, 2013; Leya *et al.*, 2009), the trigger and the process and mechanisms leading to pigment production are not fully understood. Our results show that on a single glacier and even over a short time period there is a great heterogeneity in pigment compositions, both in space (Fig. 5a) and time (Fig. 5b). This fact needs to be taken into account when pigment contents are described at a specific sampling site and time and when comparisons with other locations are made. Snow samples collected a week apart from almost the same location showed much higher secondary carotenoid contents relative to the initial samples, while esterified astaxanthin was only found in samples collected 2 weeks after melting initiation (Table 4 and Fig. 5). Although biological processes are known to occur very slowly at 0°, snow algae seem to adapt quickly to changing conditions with a broad range of pigment ratios (i.e. chlorophylls and carotenoids). Carotenoids play an important role in photo-protection by absorbing excessive photosynthetic energy, shading the chloroplast against high irradiation or as a pool of antioxidative compounds (Grossman *et al.*, 2004). Although various carotenoid pigments were identified in our samples (Table 4 and Fig. 5), and despite a good peak separation in the HPLC chromatograms, none of the xantophylls (carotenoids with oxygen functional groups) violaxanthin, zeaxanthin and antheraxanthin were found in the two green snow samples (MIT-11, MIT-22), and only a minor component of these xantophylls was found in the red snow samples. In addition, as we targeted the main snow algae pigments in our analyses, we did not find the main ice algae pigment (purpurogallin carboxylic acid-6-O-b-D-glucopyranoside), which was recently identified by Remias *et al.* (2012b). Remias *et al.* (2012a) showed that the ice alga *A. nordenskiöldii* has abundant secondary pigments. However, we did not detect any secondary carotenoids in our ice algal samples. This could be because the samples were collected at the beginning of the melting season, and ice algae may not have been exposed long enough to excessive irradiation in order to produce secondary carotenoids.

© 2014 Federation of European Microbiological Societies.
Published by John Wiley & Sons Ltd. All rights reserved

Nutrient cycling on the glacier and delivery to downstream ecosystems

Glaciers are usually considered as important nutrient deliverers for downstream ecosystems such as deglaciated soils, lakes or coastal waters (Foreman *et al.*, 2007; Hood *et al.*, 2009; Stibal *et al.*, 2012a, b). We showed here that throughout the 3 weeks of our field season, nutrients were not in excess on Mittivakkat glacier. In our observation period, nutrient concentrations in all collected and analysed snow, ice and water samples (MIT-2 to MIT-25) were overall low and this is also represented in the low nutrient values in our run-off sample (MIT-5) suggesting low nutrient export. This also indicates that any mineral dust delivered nutrients were either not bioavailable or that any delivered dust was immediately consumed by the fast growing snow and ice algae. Thus, fast nutrient re-cycling followed by nutrient retention in the microbial biomass dominated the processes observed on Mittivakkat glacier. In addition, cell counts of our run-off sample (and the lack of cells in the clean snow and ice) indicate that only very few algal cells were transported off the glacier (Table 2). Microscopy revealed that algal cells were transferred from one microbial pool to another – that is from the snow to the ice and from the snow and ice to the cryoconite holes. Thus, we hypothesize that carbon loss in form of algal cell removal is negligible on glaciers, but that snow and ice algae act as carbon sources for the bacterial communities in the later active cryoconite holes (Irvine-Fynn *et al.*, 2012). Although information on organic carbon contents or export is lacking for this glacier, the high cell and nutrient retention (Tables 2 and S2) imply a similar trend for particulate organic carbon. Cell retention is also strongly supported by the FTIR and microscopy evidence (Figs 5 and S2) which showed high contents of 'sticky' extracellular polymeric substances (primarily carbohydrates). This was specifically true for the biofilms growing at the snow-ice interface and in the red snow algae that colonized the highest reaches of the glacier. However, dissolved organic carbon (DOC) is likely to be exported off the glacier (Hood *et al.*, 2009).

Cell retention and effect on albedo

On Mittivakkat glacier, we found that the growth of snow and ice algae is the dominant process immediately upon melting onset and most snow fields transgress through a red snow to grey ice stage. The extent of the snow and ice algae coverage is also linked to the amount of stagnant water, which in turn, is strongly influenced by slope and run-off rates (Stibal *et al.*, 2012a, b). The clear positive net photosynthetic rates (i.e. assumed here as an indicative of the accumulation of organic matter) in the snow and ice samples compared with the cryoconite hole samples collected at the same time show that snow and ice algae dominate the primary production at the onset of melting. Here, we demonstrate that the growth and retention of cells at the surface of snow and ice have a strong influence on albedo. Depending on the complexity of the produced pigments (which in turn is linked to cell maturity) as well as cell density, both the green and red snow algae can reduce the albedo to values as low as 40% which is comparable with values reported by Thomas & Duval (1995). Interestingly, the rather ephemeral biofilms at the snow-ice interface reduced albedo values down to *c.* 20% (Table 3) which is comparable with albedo values for cryoconites (Takeuchi & Li, 2008; Takeuchi, 2009). The effect and role of ice algae on albedo, despite their high spatial coverage once most snow has melted, is the least well known. Our values for the grey ice were comparable with those reported by Yallop *et al.* (2012) and reached 35%. Yallop *et al.* (2012) and Cook *et al.* (2012) have suggested that ice algae may fix up to 11 times more carbon than cryoconites holes (based on dry weight of sediment). Combining the contribution of the early-season dominating snow algae and the late season dominating ice algae not just on albedo but also on primary productivity and carbon fluxes leads us to suggest that they are major players in the ecology of glaciers and ice sheets and potentially strong impact on adjacent ecosystems. A decreased albedo may have positive feedbacks on the algal community with higher and longer melting events further enhancing algal growth and most likely even extending their period of metabolic activity. However, higher cell numbers will most likely be constrained by nutrient availability, which we show to be very low in our study. Nitrogen depletion is known to trigger secondary carotenoid production what in return could be responsible for the dark red coloration of snow fields (Remias *et al.*, 2005; Leya *et al.*, 2009) reducing albedo to a greater extent. During the time of observation, the development of pigmentation was not the sole cause of the observed darkening of the glacial surface although we hypothesize here it was likely the most dramatic. Takeuchi (2009, 2013) also found that the change in spectral reflectance on an Alaskan glacier is not only due to the physical properties of the glacial surface, but also due to biological processes. However, previous studies have shown that the age of snow, which affects water content and grain size, and especially aggregation of allochtonous dust particles (e.g. dark inorganic and black carbon; Wientjes *et al.*, 2011) can also play important roles. Our observations indicate that dust probably played a minor role on the measured snow fields, whereas the

© 2014 Federation of European Microbiological Societies.
Published by John Wiley & Sons Ltd. All rights reserved

accumulation and aggregation of allochtonous materials on the bare exposed ice surface is more important. However, the relative contribution of algal pigmentation vs. dust to the grey coloration of the bare grey ice remains unknown and needs further investigation.

Acknowledgements

The authors would like to thank the anonymous reviewers for their comments that helped to improve the manuscript. The research leading to these results has received funding from INTERACT (grant agreement no. 262693), under the European Union's Seventh Framework Programme and an University of Leeds School of Earth and Environment grant to SL and LGB. We acknowledge Dr. S. Allshorn from the Cohen Laboratories at the School of Earth and Environment, University of Leeds for help with IC measurements, Dr. Gary Fones from the University of Portsmouth for the ICP-MS measurements and the Department of Geosciences and Natural Resource Management at the University of Copenhagen for provision of temperature data. The authors state no conflict of interest.

References

Anesio AM & Laybourn-Parry J (2012) Glaciers and ice sheets as a biome. *Trends Ecol Evol* **27**: 219–225.

Bidigare R, Ondrusek M, Kennicutt M, Iturriaga R, Harvey H, Hoham R & Macko S (1993) Evidence for a photoprotective function for secondary carotenoids of snow algae. *J Phycol* **29**: 427–434.

Cappelen J, Laursen EV, Jørgensen PV & Kern-Hansen C (2011) DMI monthly climate data collection 1768–2010, Denmark, The Faroe Islands and Greenland. *Technical Report 06-09*.

Christner BC, Kvitko BH & Reeve JN (2003) Molecular identification of bacteria and eukarya inhabiting an Antarctic cryoconite hole. *Extremophiles* **7**: 177–183.

Cook J, Hodson A, Anesio A, Hanna E, Yallop M, Stibal M, Telling J & Huybrechts P (2012) An improved estimate of microbially mediated carbon fluxes from the Greenland ice sheet. *J Glaciol* **58**: 1098.

de Oliveira VE, Castro HV, Edwards HG & de Oliveira LFC (2010) Carotenes and carotenoids in natural biological samples: a Raman spectroscopic analysis. *J Raman Spectrosc* **41**: 642–650.

Duval B, Duval E & Hoham RW (2010) Snow algae of the Sierra Nevada, Spain, and high Atlas mountains of Morocco. *Int Microbiol* **2**: 39–42.

Edwards A, Anesio AM, Rassner SM, Sattler B, Hubbard B, Perkins WT, Young M & Griffith GW (2010) Possible interactions between bacterial diversity, microbial activity and supraglacial hydrology of cryoconite holes in Svalbard. *ISME J* **5**: 150–160.

Escher A & Watt WS (1976) *Geology of Greenland*. Geological Survey of Greenland, Copenhagen.

Foreman CM, Sattler B, Mikucki JA, Porazinska DL & Priscu JC (2007) Metabolic activity and diversity of cryoconites in the Taylor Valley, Antarctica. *J Geophys Res* **112**: G04S32.

Fujii M, Takano Y, Kojima H, Hoshino T, Tanaka R & Fukui M (2010) Microbial community structure, pigment composition, and nitrogen source of red snow in Antarctica. *Microb Ecol* **59**: 466–475.

Gentz-Werner P (2007) *Roter Schnee: oder Die Suche nach dem färbenden Prinzip*. Akademie Verlag, Berlin.

Grossman AR, Lohr M & Im CS (2004) *Chlamydomonas reinhardtii* in the landscape of pigments. *Annu Rev Genet* **38**: 119–173.

Hanna E, Mernild SH, Cappelen J & Steffen K (2012) Recent warming in Greenland in a long-term instrumental (1881–2012) climatic context: I. Evaluation of surface air temperature records. *Environ Res Lett* **7**: 045404.

Hanna E, Fettweis X, Mernild SH, Cappelen J, Ribergaard MH, Shuman CA, Steffen K, Wood L & Mote TL (2013) Atmospheric and oceanic climate forcing of the exceptional Greenland ice sheet surface melt in summer 2012. *Int J Climatol* **7**: 045404.

Hodson A, Cameron K, Boggild C, Irvine-Fynn T, Langford H, Pearce D & Banwart S (2010) The structure, biological activity and biogeochemistry of cryoconite aggregates upon an Arctic valley glacier: Longyearbreen, Svalbard. *J Glaciol* **56**: 349–362.

Hoham R & Duval B (2001) *Microbial Ecology of Snow and Freshwater Ice with Emphasis on Snow Algae*, pp. 168–228. Cambridge University Press, Cambridge.

Hood E, Fellman J, Spencer RG, Hernes PJ, Edwards R, D'Amore D & Scott D (2009) Glaciers as a source of ancient and labile organic matter to the marine environment. *Nature* **462**: 1044–1047.

Irvine-Fynn T, Edwards A, Newton S, Langford H, Rassner S, Telling J, Anesio A & Hodson A (2012) Microbial cell budgets of an Arctic glacier surface quantified using flow cytometry. *Environ Microbiol* **14**: 2998–3012.

Leya T (2004) *Feldstudien und genetische Untersuchungen zur Kryophilie der Schneealgen Nordwestspitzbergens*. Dissertation. Shaker, Aachen.

Leya T, Müller T, Ling H & Fuhr G (2000) Taxonomy and biophysical properties of cryophilic microalgae and their environmental factors in Northwest Spitsbergen, Svalbard.

Leya T, Ling TMÃHU & Fuhr GÃ (2004) Snow algae from north-western Spitsbergen (Svalbard). *The coastal ecosystem of Kongsfjorden, Svalbard Synopsis of biological research performed at the Koldewey Station in the years 1991–2003*.

Leya T, Rahn A, Lütz C & Remias D (2009) Response of arctic snow and permafrost algae to high light and nitrogen stress

© 2014 Federation of European Microbiological Societies.
Published by John Wiley & Sons Ltd. All rights reserved

by changes in pigment composition and applied aspects for biotechnology. *FEMS Microbiol Ecol* **67**: 432–443.

Lütz C, Remias D & Holzinger A (2009) Comparative ultrastructure of snow-and ice-algae from polar and alpine habitats.

Mernild SH, Knudsen NT & Hanna E (2012) Mittivakkat Gletscher, the longest-observed mountain glacier in Greenland, experiences its fourth largest mass loss year since 1995. http://www.eu-interact.org/fileadmin/user_upload/pdf/Mittivakkat_Gletscher_2012_press_release.pdf.

Müller T, Bleiss W, Martin CD, Rogaschewski S & Fuhr G (1998) Snow algae from northwest Svalbard: their identification, distribution, pigment and nutrient content. *Polar Biol* **20**: 14–32.

Müller T, Leya T & Fuhr G (2001) Persistent snow algal fields in Spitsbergen: field observations and a hypothesis about the annual cell circulation. *Arct Antarct Alp Res* **33**: 42–51.

Nghiem S, Hall D, Mote T, Tedesco M, Albert M, Keegan K, Shuman C, DiGirolamo N & Neumann G (2012) The extreme melt across the Greenland ice sheet in 2012. *Geophys Res Lett* **39**: L20502.

Remias D, Lütz-Meindl U & Lütz C (2005) Photosynthesis, pigments and ultrastructure of the alpine snow alga *Chlamydomonas nivalis*. *Eur J Phycol* **40**: 259–268.

Remias D, Albert A & Lütz C (2010) Effects of realistically simulated elevated UV irradiation on photosynthesis and pigment composition of the alpine snow alga *Chlamydomonas nivalis* and the arctic soil alga *Tetracystis* sp. (Chlorophyceae). *Photosynthetica* **48**: 269–277.

Remias D, Holzinger A, Aigner S & Lütz C (2012a) Ecophysiology and ultrastructure of *Ancylonema nordenskiöldii* (Zygnematales, Streptophyta), causing brown ice on glaciers in Svalbard (high arctic). *Polar Biol* **35**: 1–10.

Remias D, Schwaiger S, Aigner S, Leya T, Stuppner H & Lütz C (2012b) Characterization of an UV-and VIS-absorbing, purpurogallin-derived secondary pigment new to algae and highly abundant in *Mesotaenium berggrenii* (Zygnematophyceae, Chlorophyta), an extremophyte living on glaciers. *FEMS Microbiol Ecol* **79**: 638–648.

Remias D, Wastian H, Lütz C & Leya T (2013) Insights into the biology and phylogeny of *Chloromonas polyptera* (Chlorophyta), an alga causing orange snow in Maritime Antarctica. *Antarct Sci* **25**: 648–656.

Säwström C, Mumford P, Marshall W, Hodson A & Laybourn-Parry J (2002) The microbial communities and primary productivity of cryoconite holes in an Arctic glacier (Svalbard 79 N). *Polar Biol* **25**: 591–596.

Siddiqui KS & Cavicchioli R (2006) Cold-adapted enzymes. *Annu Rev Biochem* **75**: 403–433.

Stibal M, Elster J, Šabacká M & Kaštovská K (2007) Seasonal and diel changes in photosynthetic activity of the snow alga *Chlamydomonas nivalis* (Chlorophyceae) from Svalbard determined by pulse amplitude modulation fluorometry. *FEMS Microbiol Ecol* **59**: 265–273.

Stibal M, Tranter M, Benning LG & Řehák J (2008) Microbial primary production on an Arctic glacier is insignificant in comparison with allochthonous organic carbon input. *Environ Microbiol* **10**: 2172–2178.

Stibal M, Šabacká M & Žárský J (2012a) Biological processes on glacier and ice sheet surfaces. *Nat Geosci* **5**: 771–774.

Stibal M, Telling J, Cook J, Mak KM, Hodson A & Anesio AM (2012b) Environmental controls on microbial abundance and activity on the Greenland ice sheet: a multivariate analysis approach. *Microb Ecol* **63**: 74–84.

Takeuchi N (2009) Temporal and spatial variations in spectral reflectance and characteristics of surface dust on Gulkana Glacier, Alaska Range. *J Glaciol* **55**: 701–709.

Takeuchi N (2013) Seasonal and altitudinal variations in snow algal communities on an Alaskan glacier (Gulkana glacier in the Alaska range). *Environ Res Lett* **8**: 035002.

Takeuchi N & Li Z (2008) Characteristics of surface dust on Ürümqi glacier No. 1 in the Tien Shan Mountains, China. *Arct Antarct Alp Res* **40**: 744–750.

Takeuchi N, Uetake J, Fujita K, Aizen VB & Nikitin SD (2006) A snow algal community on Akkem glacier in the Russian Altai Mountains. *Ann Glaciol* **43**: 378–384.

Tedesco M, Fettweis X, Mote T, Wahr J, Alexander P, Box J & Wouters B (2013) Evidence and analysis of 2012 Greenland records from spaceborne observations, a regional climate model and reanalysis data. *The Cryosphere* **7**: 615–630.

Telling J, Anesio AM, Tranter M, Irvine-Fynn T, Hodson A, Butler C & Wadham J (2011) Nitrogen fixation on Arctic glaciers, Svalbard. *J Geophys Res* **116**: G03039.

Thomas WH & Duval B (1995) Sierra Nevada, California, USA, snow algae: snow albedo changes, algal-bacterial interrelationships, and ultraviolet radiation effects. *Arct Alp Res* **27**: 389–399.

Wientjes I, Van de Wal R, Reichart G-J, Sluijs A & Oerlemans J (2011) Dust from the dark region in the western ablation zone of the Greenland ice sheet. *Cryosphere* **5**: 589–601.

Williams WE, Gorton HL & Vogelmann TC (2003) Surface gas-exchange processes of snow algae. *P Natl Acad Sci USA* **100**: 562–566.

Yallop ML, Anesio AM, Perkins RG, Cook J, Telling J, Fagan D, MacFarlane J, Stibal M, Barker G & Bellas C (2012) Photophysiology and albedo-changing potential of the ice algal community on the surface of the Greenland ice sheet. *ISME J* **6**: 2302–2313.

Supporting Information

Additional Supporting Information may be found in the online version of this article:

Data S1. Methods.

Fig. S1. Raman spectra of three different cell types: ice algae (blue), red mature snow algae (red) and young green snow algae (green).

Fig. S2. SEM micrographs of *Chlamydomonas* cell morphologies, smooth (a), with some nipples (b, c), shrivelled (d), wave-like structures (f), highly covered with

© 2014 Federation of European Microbiological Societies.
Published by John Wiley & Sons Ltd. All rights reserved

minerals with a diatom (g), biofilm with *Chlamydomonas* and *Ancylonema* (e, h, i).

Fig. S3. TEM photomicrographs of *Chlamydomonas* (1–4) and *Ancylonema* (5) cells.

Table S1. Albedo measurements across the 1-km^2 area shown in Fig. 1 main text with coordinates and 10 measurements per site; the five up and down values represent five incident and five reflected radiation measurements at each point.

Table S2. Aqueous chemical analyses of anions and cations by IC and ICP-MS in all samples.

Table S3. Raman spectroscopy analyses of (a) minerals and black carbon in the three samples and (b) organic compounds.

© 2014 Federation of European Microbiological Societies.
Published by John Wiley & Sons Ltd. All rights reserved